Selective Metal-Assisted Oxidative Cleavage of a C−N Bond: Synthesis and Characterization of the Mononuclear Iron(III) [Fe(BPG)Cl_2] Complex and Its Two [Fe(BPA)Cl_3] and [Fe(BPE)Cl_3] Derivatives†

Marie-Carmen Rodriguez, François Lambert, and Irène Morgenstern-Badarau*

Laboratoire de Chimie Bioorganique et Bioinorganique, Institut de Chimie Moléculaire d'Orsay, Université Paris-Sud, 91405 Orsay, France

Michèle Cesario and Jean Guilhem

Institut de Chimie des Substances Naturelles, CNRS, 91198 Gif-s/-Yvette, France

Bineta Keita and Louis Nadjo

Laboratoire d'Electrochimie et de Photoélectrochimie, Institut de Chimie Moléculaire d'Orsay, Université Paris-Sud, 91405 Orsay, France

Received November 14, 1996⊗

A new example of a site-selective metal-assisted oxidative cleavage of a C−N bond is reported. This phenomenon occurs in the nitrogen-centered tetradentate tripodal BPG ligand (BPG = (bis(2-pyridylmethyl)amino)acetate), which combines one carboxylate and two pyridines as pendant groups, when coordinated to iron(III). The corresponding iron(III) [Fe(BPG)Cl_2] complex (**1**) is transformed to the iron(III) [Fe(BPA)Cl_3] complex (**2**) with the tridentate BPA ligand (BPA = bis(2-pyridylmethyl)amine) retaining only two pyridine pendant groups, while the initial BPG carboxylate group is transformed to glyoxylic acid. The [Fe(BPA)Cl_3] complex (**2**) has been fully characterized as well as another, [Fe(BPE)Cl_3] (**3**), formed with the tridentate BPE ligand (BPE = methyl (bis(2-pyridylmethyl)amino)acetate) which, in addition to two pyridines, presents an ester group. The crystal structures of these two complexes have been resolved. The asymmetric unit of complex **2** has been characterized by two mononuclear neutral molecules linked by two hydrogen bonds. (Crystal data for **2**: orthorhombic, $Pna2_1$, $a = 15.603(8)$ Å, $b = 8.485(4)$ Å, $c = 22.752(11)$ Å, $\alpha = \beta = \gamma = 90°$, $V = 3012(3)$ Å^3, $Z = 8$, $R = 0.0582$ [2813 reflections with $I > 2\sigma(I)$], and $R_w = 0.1430$.) Complex **3** is symmetric with the iron center, the amine nitrogen, one choride and the three atoms of the carboxylate group in special positions in the mirror plane. (Crystal data for **3**: orthorhombic, $Pmn2_1$, $a = 10.418(4)$ Å, $b = 12.952(5)$ Å, $c = 7.353(3)$ Å, $\alpha = \beta = \gamma = 90°$, $V = 992.2(7)$ Å^3, $Z = 2$, $R = 0.0500$ [513 reflections with $I > 2\sigma(I)$], and $R_w = 0.1231$.) Redox potentials corroborate the structural features ($E° = -38$ mV for **1**, -19 mV for **2**, and $+145$ mV for **3** *vs* SCE in acetonitrile). Preliminary studies of the [Fe(BPG)Cl_2] complex have shown that it reacts in its reduced form with dioxygen.

Introduction

Model systems that mimic active sites of metalloproteins are important mechanistic tools, since their properties can be adjusted by suitably modifying the ligand units. More specifically and within the last decade, in the case of non-heme iron proteins, a good deal of effort has been made in the synthesis of low molecular weight complexes formed with a variety of ligands to model the function and/or the spectroscopic features. Moreover, according to structural information now available, similar metal environments can correspond to different functions. For example, this is the case for the diiron center in methane monooxygenase[1a,2] and ribonucleotide reductase,[1b,c,2] as well as for the mononuclear iron site in soybean lipoxygenase[3] and iron superoxide dismutase.[4] Modeling studies of the chemistry of these enzymes might provide features of key transient species involved in the proposed mechanisms and could differentiate their modes of reactivity.

As part of our study of the reaction of synthetic mononuclear non-heme iron complexes with dioxygen and its derivatives, we first focused on iron(III) model compounds for the iron superoxide dismutase and the lipoxygenase. Their common structural features at the active site are three histidines and one carboxylate ligand. In addition to this N_3O_1 set of donor atoms,

* To whom correspondence should be addressed. Tel.: 33-1-69157831. Fax: 33-1-69157281. E-mail: imorgens@icmo.u-psud.fr.

† Abbreviations used: BPG, (bis(2-pyridylmethyl)amino)acetate; BPA, bis(2-pyridylmethyl)amine; BPE, methyl(bis(2-pyridylmethyl)amino)acetate; Hbpp, 3-[bis(2-pyridylmethyl)amino]propionic acid.

⊗ Abstract published in *Advance ACS Abstracts,* July 1, 1997.

(1) (a) Rosenzweig, A. C.; Frederick, C. A.; Lippard, S. J.; Nordlund, P. *Nature* **1993**, *366*, 537. (b) Nordlund, P.; Sjöberg, B. M.; Erlund, H. *Nature* **1990,** *345*, 593−598. (c) Nordlung, P.; Eklund, H. *J. Mol. Biol.* **1993**, *232*, 123−164.

(2) See for example: (a) Vincent, J. B.; Olivier-Lilley, G. L.; Averill, B. A. *Chem. Rev.* **1990**, *90*, 1447−1467. (b) Feig, A. L.; Lippard, S. J. *Chem. Rev.* **1994**, *94*, 759−805. (c) Que, L., Jr.; Dong, Y. *Acc. Chem. Res.* **1996**, *29*, 190−196.

(3) (a) Boyington, J. C.; Gaffney, B. J.; Amzel, L. M. *Science* **1993**, *260*, 1482−1486. (b) Minor, W.; Steczko, J.; Bolin, J. T.; Otwinowski, Z.; Axelrod, B. *Biochemistry* **1993**, *32*, 6320−6323.

(4) (a) Stoddard, B. L.; Howell, P. L.; Ringe, D.; Petsko, G. A. *Biochemistry* **1990**, *29*, 8885. (b) Tierney, D. L.; Fee, J. A.; Ludwig, M. L.; Penner-Hahn, J. E. *Biochemistry* **1995**, *34*, 1661−1668. (c) Stallings, W. C.; Pattridge, K. A.; Strong, R. K.; Ludwig, M. L. *J. Biol. Chem.* **1985**, *260*, 16424−16432. (d) Stalling, W. C.; Metzger, A. L.; Pattridge, K. A.; Fee, J. A.; Ludwig, M. L. *Free Radicals Res. Commun.* **1991**, *12*−13, 259−268.

S0020-1669(96)01369-9 CCC: $14.00

Chart 1

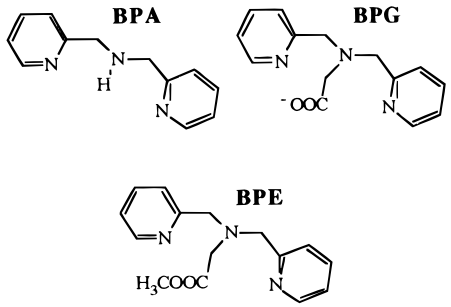

the iron center is also likely to be bound to a fifth ligand, a water molecule or an asparagine residue, respectively.[3b,4] We therefore undertook the synthesis of a series of closely related tripodal tetradentate ligands derived from the structural pattern $N(CH_2R)_3$. The iron environment varies systematically when two of the pendant groups are either pyridine or imidazole groups representing the histidines, while the third one remains a carboxylic acid which accounts for the carboxylate ligand of the active sites. We have succeeded in the synthesis of two new tripodal tetradentate ligands, combining imidazole functions and an acid function. In addition to the carboxylate pendant group, one of them contains two imidazole pendant groups and the other contains one imidazole and one pyridine. The route to their synthesis as well as the structure and chemical properties of the corresponding chloride iron(III) complexes are reported elsewhere.[5]

For the sake of comparison, we were also interested in the investigation of the mononuclear iron(III) complex of the tripodal tetradentate ligand (bis(2-pyridylmethyl)amino)acetic acid (BPGH) (Chart 1), which contains two pyridine and one acid pendant groups. The synthesis of this ligand and the corresponding iron(III)−catecholate complexes were previously reported.[6] A closely related ligand Hbpp[†] with a longer carboxylate arm has been proposed for the synthesis of dinuclear iron complexes.[7] Insofar as BPGH had already been used for modeling mononuclear non-heme iron active sites, we expected this ligand to coordinate the iron without further reaction. However, we discovered the situation to be far more intricate. In fact, we obtained the following three different complexes depending on the synthesis conditions, $[Fe(BPG)Cl_2]$ (**1**), $[Fe(BPA)Cl_3]$ (**2**), and $[Fe(BPE)Cl_3]$ (**3**), in which BPG, BPA, and BPE are the ligands presented in Chart 1. Thus when allowed to stay in solution, the BPG ligand undergoes a site-selective, metal-assisted, oxidative cleavage of a C−N bond, to yield the corresponding BPA amine, and can be esterified to give the BPE ligand.

Ligand oxidations have already been reported. For example, oxidative dehydrogenation of secondary amine functions coordinated to iron(II) or iron(III) have been investigated.[8] Reaction with dioxygen of bis(β-diimine) macrocycle ligands or imidazole groups coordinated to iron(II) and cobalt(III) to yield complexes containing carbonyl functions have also been described.[9] Site selective cleavage of C−N bonds has been observed in the case of coordinated polyamines[9,10] and tertiary amines.[11] For example, site-selective oxidation of spermine has been observed in a cobalt(III) spermine complex that results in a C−N cleavage. Under acidic conditions, $Co(trpn)(H_2O)_2$ [trpn = tris-(3-aminopropyl)amine] completely converts into Co(II) and organic byproducts resulting from bis(3-aminopropyl)amine and $NH_2CH_2CH_2CHO$. Such reactions are of interest for the understanding of the oxidative dealkylation catalyzed by cytochrome P450.[12]

In this paper, we report the synthesis and characterization of the three iron(III) complexes mentioned above. The crystal structures of two, $[Fe(BPA)Cl_3]$ and $[Fe(BPE)Cl_3]$, have been resolved. Evidence of the oxidative cleavage is clearly established, and possible mechanisms are proposed. We also report preliminary experiments which give insight into their reactivities within our program to investigate new mononuclear non-heme iron models probably involved in dioxygen activation.[5]

Experimental Section

Materials and Synthesis. 2-(Aminomethyl)pyridine, 99%, 2-pyridinecarboxaldehyde, 99%, ethyl bromocetate, 97%, and $FeCl_3 \cdot 6H_2O$ were purchased from Jansen Chimica.

All solvents were of reagent grade and used without further purification except when indicated in which case solvents were dried by standard procedures.

Bis(2-pyridylmethyl)amine (BPA) was synthesized by following the published method.[13] ^{1}H NMR (in $CDCl_3$), ppm: 3.93 (s, 4H, N−CH_2−Py); 7.12 (m, 2H, H_{Py}); 7.34 (m, 2H, H_{Py}); 7.6 (m, 2H, H_{Py}); 8.5 (m, 2H, H_{6-Py}). ^{13}C NMR (in D_2O), ppm: 54.60 (2C, N−CH_2−Py); 121.90 (2C, C_{5-Py}); 122.25 (2C, C_{3-Py}); 136.40 (2C, C_{4-Py}); 149.20 (2C, C_{6-Py}); 159.45 (2C, C_{2-Py}).

(Bis(2-pyridylmethyl)amino)acetic Acid (BPGH). This ligand was synthesized according to a modified literature procedure.[6b] To a solution of bis(2-pyridylmethyl)amine (BPA) (3 g, 15 mmol) in anhydrous dimethylformamide (40 mL) were added potassium carbonate (8.07 g, 15 mmol) and ethyl bromoacetate (1.66 mL, 15 mmol), under argon. The resulting suspension was protected from light and allowed to stir at 30 °C, under argon, for 32 h. After filtration the solvent was evaporated and the resulting red oil was purified by gel chromatography. A dichloromethane/methanol (95:5) solution was used as eluant to give 2.65 g of (ethoxycarbonyl)ethyl)bis(2-pyridylmethyl)amine (yield 62%). The BPGH ligand was obtained by hydrolysis of the ester and subsequent acidification. To a solution of (ethoxycarbonyl)ethyl)bis-(2-pyridylmethyl)amine (1.4 g, 5 mmol) in methanol (30 mL) was added a solution of potassium carbonate (1.6 g, 11.5 mmol) in water (60 mL). The resulting solution was allowed to stir for 5 days at room temperature. The solvent was then half-evaporated and washed by 3 × 20 mL of dichloromethane. An aqueous solution of hydrochloric

(5) (a) Rodriguez, M-C.; Morgenstern-Badarau, I.; Cesario, M.; Guilhem, J.; Keita, B.; Nadjo, L. *Inorg. Chem.* **1996**, *35*, 7804−7810. (b) Rodriguez, M.-C.; Morgenstern-Badarau, I. To be submitted for publication.

(6) (a) Cox, D. D.; Benkovic, S. J.; Bloom, L. M.; Bradley, F. C.; Nelson, M. J.; Que, L., Jr.; Wallick, D. E. *J. Am. Chem. Soc.* **1988**, *110*, 2026−3032. (b) Cox, D. D.; Que, L., Jr. *J. Am. Chem. Soc.* **1988**, *110*, 8085−8092.

(7) Hazell, A.; Jensen, K. B.; McKenzie, C. J.; Toftlund, H. J. *J. Chem. Soc., Dalton Trans.* **1993**, 3249−3257.

(8) (a) Kuroda, Y.; Tanaka, N.; Goto, M.; Sakai, T. *Inorg Chem.* **1989**, *28*, 2163. (b) Goto, M.; Takeshita, M.; Kanda, N.; Sakai, T. *Inorg. Chem.* **1985**, *24*, 582. (c) Mehne, L. F.; Wayland, B. B. *Inorg. Chem.* **1975**, *14*, 881−885. (d) Goedken, V. L.; Bush, D. H. *J. Am. Chem. Soc.* **1972**, *94*, 7355−7363.

(9) (a) Weiss, M. C.; Goedken, V. L. *J. Am. Chem. Soc.* **1976**, *98*, 3389−3392. (b) Switzer, J. A.; Endicott, J. F. *J. Am. Chem. Soc.* **1980**, *102*, 1181. (c) Riley, D. P.; Busch, D. H. *Inorg. Chem.* **1983**, *22*, 4141. (d) Guillot, G.; Mulliez, E.; Leduc, P.; Chottard, J.-C. *Inorg. Chem.* 1**990**, *29*, 577.

(10) (a) Arulsamy, N.; Hogson, D. J. *Inorg. Chem.* **1994**, *33*, 453. (b) Yashiro, M.; Mori, T.; Sekiguchi, M.; Yoshikawa, S.; Shiraishi, S. *J. Chem Soc., Chem. Commun.* **1992**, 1167−1168. (c) Sonnberger, B.; Hühn, P.; Wasserburger, A.; Wasgestein, F. *Inorg. Chim. Acta* **1992**, *196*, 65−71.

(11) (a) Riley, D. P.; Fields, D. L.; Rivers, W. *J. Am Chem. Soc.* **1991**, *113*, 3371−3378. (b) Sanyal, I.; Mahroof-Tahir, M.; Nasir, M. S.; Ghosh, P.; Cohen, B. I.; Gulneth, Y.; Cruse, R. W.; Farooq, A.; Karlin, K. D.; Liu, S.; Zubieta, J. *Inorg. Chem.* **1992**, *31*, 4322−4332. (c) Calafat, A. M.; Marzilli, L. G. *Inorg. Chem.* **1993**, *32*, 2906−2911. (d) Riley, D. P.; Fields, D. L.; Rivers, W. *Inorg. Chem.* **1991**, *30*, 4191−4197.

(12) Karki, S. B.; Dinnocenzo, J. P.; Jones, J. P.; Korzekwa, K. R. *J. Am. Chem. Soc.* **1995**, *117*, 3657−3664.

(13) Gruenwedel, D. W. *Inorg. Chem.* **1968,** *3*, 495−501.

acid (230 mL, 23 mmol, 0.1 M) was then added and the product lyophilized. The resulting powder was extracted by anhydrous methanol. Addition of diethyl ether at low temperature allowed the final product to precipitate as hygroscopic crystals (yield 46%). ^{1}H NMR (in D_2O), ppm: 3.45 (s, 2H, N−*CH2*−COOH); 4.15 (s, 4H, N−CH2−Py); 7.25 (m, 4H, H_{Py}); 7.70 (m, 2H, H_{Py}); 8.25 (m, 2H, H_{Py}). ^{13}C NMR (in D_2O), ppm: 58.4 (1C, *CH*$_2$−COOH); 58.8 (2C, CH_2−Py); 125.6 (2C, C_{5-Py}); 126.1 (2C, C_{3-Py}); 141.7 (2C, C_{4-Py}); 147.9 (2C, C_{6-Py}); 152.3 (2C, C_{2-Py}); 174.8 (1C, COOH).

[Fe(BPG)Cl$_2$] (1). The complex was obtained by mixing a solution of BPGH (128.6 g, 0.5 mmol) and piperidine (12 μL, 0.125 mmol) in anhydrous methanol (10 mL) and a solution of $FeCl_3 \cdot 6H_2O$ (0,135 g, 0.5 mmol) in anhydrous methanol (10 mL) under argon. The yellow precipitate obtained by heating the resulting solution for 5 min was filtrated out, washed with anhydrous methanol (10 mL), and vacuum-dried (yield 75%). Anal. Calcd for $C_{14}H_{14}N_3FeCl_2O_2$: C, 43.90; H, 3.68; N, 10.96; Fe, 14.58; Cl, 18.51. Found: C, 43.89; H, 3.7; N, 10.69; Fe, 14.06; Cl, 18.55.

[Fe(BPA)Cl$_3$] (2). To a solution of BPGH (128.6 g, 0.5 mmol) and piperidine (25 μL, 0.25 mmol) in 10 mL of a methanol/acetonitrile (1/1) mixture was added a solution of $FeCl_3 \cdot 6H_2O$ (0.135 g, 0.5 mmol) in the same solvent with stirring under argon. The resulting solution was refluxed for 30 min. Methanol was then allowed to diffuse in the resulting yellow solution for 2 weeks to yield yellow-orange crystals suitable for X-ray analysis (yield 80%). Anal. Calcd for $C_{12}H_{13}N_3FeCl_3$: C, 39.8; H, 3.62; N, 11.62; Cl, 29.42. Found: C, 39.91; H, 3.65; N, 11.75; Cl, 29.29.

[Fe(BPE)Cl$_3$] (3). To a solution of BPGH (146.5 g, 0.5 mmol) in methanol (10 mL) was added a solution of $FeCl_3 \cdot 6H_2O$ (0.135 g, 0.5 mmol) in methanol (5 mL) with stirring under argon. The solution was refluxed for 30 min and then allowed to evaporate under argon for week to give yellow crystals suitable for X-ray analysis (yield 60%). Anal. Calcd for $C_{15}H_{18}N_3O_2FeCl_3$: C, 41.55; H, 3.95; N, 9.69; Cl, 24.53. Found: C, 41.6; H, 4.2; N, 9.18; Cl, 23.45.

Physical Methods. Electronic UV−vis spectra were recorded on a Safas double mode spectrophotometer in DMF or acetonitrile. Infrared spectra were recorded on a FTIR Bruker spectrophotometer as KBr disks. ^{1}H NMR and ^{13}C NMR spectra were obtained on a Bruker 200 spectrometer. Chemical shifts (in ppm) are given taking the residual protic solvent peaks as reference. GC mass spectra were recorded with a Varian 3500GC equipped with a CPSIL5 column and a Nermag R 1010 mass spectrometer.

Electrochemical Experiments. All the chemicals were of high-purity grade. CH_3CN (Prolabo, water < 0.005%) was used without further purification and kept in a glovebox under argon atmosphere prior to use. Compound Bu_4NPF_6 (Aldrich) was dried at 80 °C under vacuum for 3 days. For anaerobic conditions, the solutions were deaerated thoroughly for at least 30 min with pure argon and kept under positive pressure during the experiments. Otherwise, the solutions were saturated with air (N 50 Air Liquide) or with pure dioxygen (N 48 Air Liquide). Cyclic voltammograms were recorded with an EG G273A electrochemical analyzer driven by a PC with the 270 software, using a freshly polished glassy carbon disk (GC, Tokai, Japan, 3 mm diameter) as the working electrode, a large-surfaced platinum gauze as the auxiliary electrode, and a SCE reference electrode. The reference electrode was kept in a compartment containing the appropriate supporting electrolyte (Bu_4NPF_6) and separated from the working electrode compartment by a fine-porosity glass frit.

Crystallographic Studies. X-ray diffraction data were collected on a yellow-orange crystal of **2** of 0.03 × 0.50 × 0.80 mm^3 and a yellow crystal of **3** of 0.20 × 0.40 × 0.80 mm^3 at room temperature (293 K) on a Phillips PW 1100 diffractometer equipped with a molybdenum tube and a graphite monochromator. Crystallographic and experimental parameters are presented in Table 1. The structures were solved by direct methods, program SHELXS-86,[14a] and refined on F^2 for all reflections by the least-squares method, using SHELXL-93.[14b]

(14) (a) Sheldrick, G. M. SHELXS-86, Program for the solution of crystal structures, Göttingen, Germany, 1986. (b) Sheldrick, G. M. SHELXL-93, Göttingen, Germany, 1993. (c) Parkin, S.; Moezzi, B.; Hope, H. XABS2. *J. Appl. Crystallogr.* **1995**, *28*, 53−56.

Table 1. Crystallographic Data for [Fe(BPA)Cl$_3$] (**2**) and [Fe(BPE)Cl$_3$] (**3**)

	[Fe(BPA)Cl$_3$]	[Fe(BPE)Cl$_3$]
formula	$C_{12}H_{13}N_3FeCl_3$	$C_{15}H_{17}N_3FeCl_3O_2 \cdot H_2O$
fw	361.45	451.52
cryst system	orthorhombic	orthorhombic
space group	*Pna*21	*Pmn*21
a (Å)	15.603(8)	10.418(4)
b (Å)	8.485(4)	12.952(5)
c (Å)	22.752(11)	7.353(3)
$\alpha = \beta = \gamma$ (deg)	90.00	90.00
V (Å^3)	3012(3)	992.2(7)
Z	8	2
D_x (g/cm^{-3})	1.594	1.511
T (K)	293	293
λ (Å)	0.710 73	0.710 73
μ (mm^{-1})	1.52	1.182
R	0.0582 [2813; $I > 2\sigma(I)$]	0.0500 [513; $I > 2\sigma(I)$]
R_w	0.1430	0.1231

[Fe(BPA)Cl$_3$] (2). The complex crystallizes in the orthorhombic *Pna*2$_1$ space group with two molecules per asymmetric unit. The two molecular entities are related by a pseudo and not crystallographic center of symmetry. An empirical absorption correction (XABS2),[14c] based on minimization of differences between F_o^2 and F_c^2, was applied. H atoms were not located on difference synthesis but introduced in the refinement at theoretical positions and assigned an isotropic thermal parameter a factor of 1.1 times that of the bonded atom.

[Fe(BPE)Cl$_3$] (3). Complex **3** crystallizes in the orthorhombic *Pmn*2$_1$ space group with the molecule using the crystallographic mirror plane. H atoms were refined as riding models at theoretical positions and assigned an isotropic thermal parameter a factor 1.1 times that of the bonded atom. The only Fe and Cl atoms were refined anisotropically to limit the number of parameters *versus* the small number of data.

Results and Discussion

Syntheses. When BPGH and $FeCl_3 \cdot 6H_2O$ were reacted in methanol, in the presence of 0.5 equiv of base, a yellow powder precipitated almost immediately. The complex obtained was stable to air and was identified as the [Fe(BPG)Cl$_2$] complex where the ligand is chelated to the iron in a tetradentate way. Attempts to obtain diffraction-quality crystals of this compound were unsuccessful. We discovered side reactions that made the complex unstable in solution during the long delay necessary for good crystallization.

In order to increase the solubility of the compound and to obtain the required crystals, we used a slightly different route of synthesis whereby methanol was replaced by a mixture of methanol and acetonitrile. Instead of the [Fe(BPG)Cl$_2$] complex (**1**), we obtained new yellow-orange single crystals. Physical characterization and crystal structure described above showed that the ligand "switched" from tetradentate to tridentate by loss of one of the pendant groups to yield the [Fe(BPA)Cl$_3$] complex (**2**), thus providing a major proof for the N-dealkylation phenomenon of the BPG ligand where the N−CH_2COO bond was cleaved to yield an N−H secondary amine. This cleavage is selective in that it does not occur with the N−CH_2Py bond in which the same CH_2−N(tertiary) bond is present. Therefore, when the complex is immediately precipitated in methanol, the carboxylate group remains chelated to the iron. On the other hand, when the compound is allowed to stay in solution, a cleavage reaction can occur. It can be suggested that this reaction is metal-assisted since the ligand must first be coordinated to the iron for subsequent cleavage to occur. This was definitely confirmed when we isolated the [Fe(BPE)Cl$_3$] complex (**3**) with the ligand bound in only a tridentate way. Indeed, when the synthesis was carried out under more acidic conditions, that is with BPGH without extra addition of base,

Table 2. UV−Vis Spectral Data for the Complexes [λ, nm (ϵ, M^{-1} cm^{-1})]

	[Fe(BPG)Cl_2] (**1**)	[Fe(BPA)Cl_3] (**2**)	[Fe(BPE)Cl_3] (**3**)
CH_2Cl_2	256.5 (9550)[a]	254 (3570)	256.5 (11050)
	311 (4310)	282 (1890), sh	290.5 (5742), sh
	355.5 (3050)	381.5 (1500)	390.5 (3690)
CH_3CN	252.5 (19 760)	252 (18 550)	253.5 (13 400)
	303 (7140), sh	282 (9360), sh	293.5 (6820), sh
	350.5 (4800), sh	376.5 (6180)	383.5 (4230)
DMF	269.5 (8630)	269.5 (7150)	268 (8640)
	316.5 (6760)	310.5 (3550), sh	296 (3704), sh
	347 (4110), sh	355.5 (2608), sh	
DMSO	262 (10 140)	264.5 (11 710)	264.5 (16 000)
	305 (5170), sh	318 (4720), sh	355.5 (4980)
		358 (4170), sh	

[a] Data in parentheses are extinction coefficients.

the ligand underwent esterification by reaction with the solvent and thus was not cleaved. The [Fe(BPE)Cl_3] complex is very stable even when allowed to stay in acetonitrile for a week in the presence of dioxygen. This leads us to conclude that oxidative N-dealkylation of the coordinated ligand can be observed only when the carboxylate group is present, thus confirming the metal-assisted reaction.

IR and Electronic Absorption Properties. An IR study of [Fe(BPG)Cl_2] is very useful for better insight into the possible acetate coordination, since no X-ray structure of this complex is available. A typical ionic acetate group displays ν(C═O) and ν(C−O) stretching bands at 1578 and 1414 cm^{-1}. Upon coordination, the Δ value [ν_{as}(C═O) − ν_s(O−C−O)] is a good criterion of the binding mode of an acetate group.[15] Here [Fe(BPG)Cl_2] exhibits a broad absorption at 1667 cm^{-1} (ν_{as}(C═O)) and a lesser one at 1339 cm^{-1} (ν_s(O−C−O)) corresponding to the two vibrations of the carboxylate group. Thus, in the present case, the Δ value (328 cm^{-1}), being greater than 200 cm^{-1}, excludes the possibility of a bidentate coordination (usual value 40−80 cm^{-1}). We can assume that the carboxylate group is tethered in a monodentate way. These two absorption maxima are absent from the IR spectra of the [Fe(BPA)Cl_3] complex, but the presence of the N−H group is indicated by a sharp and intense absorption maximum at 3239 cm^{-1}. The IR spectrum of the [Fe(BPE)Cl_3] complex is also characterized by the two −COO strong absorptions at 1733 (ν_{as}) and 1277 (ν_s) cm^{-1} which indicate the presence of an ester group.

The electronic spectra were measured on solutions of freshly dissolved complexes in dimethyl sulfoxide, acetonitrile, dimethylformamide, and dichloromethane. Wavelengths of absorption maxima and corresponding molar absorbances are given in Table 2. High-energy transitions (250−400 nm) are found for all complexes. Near 260 nm, the observed strong absorption is due to the $\pi-\pi^*$ transition of the pyridine group. The other transitions show solvent dependence. They can be assigned as charge-transfer transitions with energies depending on solvent-coordinating properties. As an example, the three spectra recorded in acetonitrile are given in Figure 1.

Crystal Structures. The crystal structures of the [Fe(BPA)Cl_3] and [Fe(BPE)Cl_3] complexes reveal mononuclear neutral molecules. Selected bond distances and bond angles are listed in Tables 3 and 4. ORTEP views showing the atom-labeling scheme are presented in Figures 2 and 3. In both structures the iron(III) center is in a distorted octahedral environment consisting of two pyridine nitrogens and an amine nitrogen from the tridentate ligands and three chloride anions, with each chloride being trans to a nitrogen atom.

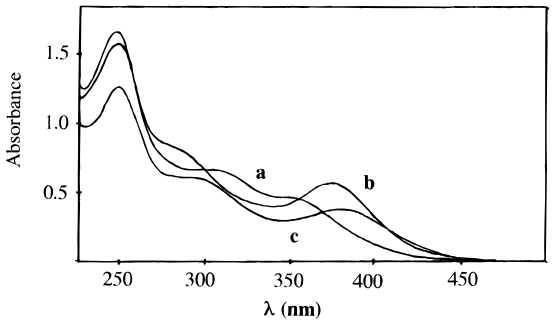

Figure 1. UV−vis absorption spectra in acetonitrile: (a) [Fe(BPG)Cl_2]; (b) [Fe(BPA)Cl_3]; (c) [Fe(BPE)Cl_3].

Table 3. Selected Bond Lengths (Å) and Angles (deg) for [Fe(BPA)Cl_3] (**2**)

Bond Lengths			
Fe−N	2.223(7)	Fe′−N′	2.197(6)
Fe−N(1A)	2.189(6)	Fe′−N(1A′)	2.185(6)
Fe−N(1B)	2.175(6)	Fe′−N(1B′)	2.214(5)
Fe−Cl(1)	2.289(3)	Fe′−Cl(1′)	2.287(3)
Fe−Cl(2)	2.327(3)	Fe′−Cl(2′)	2.312(2)
Fe−Cl(3)	2.267(2)	Fe′−Cl(3)′	2.289(2)
Bond Angles			
N−Fe−N(1A)	76.0(2)	N′−Fe′−N(1A′)	76.7(2)
N−Fe−N(1B)	76.5(3)	N′−Fe′−N(1B′)	76.8(2)
N−Fe−Cl(1)	88.9(2)	N′−Fe′−Cl(1′)	89.0(2)
N−Fe−Cl(2)	89.8(2)	N′−Fe′−Cl(2′)	91.2(2)
N−Fe−Cl(3)	167.7(2)	N′−Fe′−Cl(3′)	166.8(2)
N(1A)−Fe−N(1B)	79.0(2)	N(1A′)−Fe′−N(1B′)	79.5(2)
N(1A)−Fe−Cl(1)	164.0(2)	N(1A′)−Fe′−Cl(1′)	164.8(2)
N(1A)−Fe−Cl(2)	87.1(2)	N(1A′)−Fe′−Cl(2′)	87.5(2)
N(1A)−Fe−Cl(3)	94.7(2)	N(1A′)−Fe′−Cl(3′)	94.6(2)
N(1B)−Fe−Cl(1)	92.3(2)	N(1B′)−Fe′−Cl(1′)	92.48(14)
N(1B)−Fe−Cl(2)	162.4(2)	N(1B′)−Fe′−Cl(2′)	163.93(14)
N(1B)−Fe−Cl(3)	94.0(2)	N(1B′)−Fe′−Cl(3′)	91.92(14)
Cl(1)−Fe−Cl(2)	98.52(9)	Cl(1′)−Fe′−Cl(2′)	97.97(8)
Cl(3)−Fe−Cl(1)	99.36(9)	Cl(3′)−Fe′−Cl(1′)	98.55(8)
Cl(3)−Fe−Cl(2)	97.86(10)	Cl(3′)−Fe′−Cl(2′)	98.52(10)

Table 4. Selected Bond Lengths (Å) and Angles (deg) for [Fe(BPE)Cl_3] (**3**)[a]

Bond Lengths			
Fe−N	2.337(11)	Fe−Cl(1)	2.285(3)
Fe−N(1A)	2.194(8)	Fe−Cl(1)[1]	2.285(3)
Fe−N(1A)[1]	2.194(8)	Fe−Cl(2)	2.269(4)
Bond Angles			
N−Fe−N(1A)	75.0(3)	N(1A) −Fe−Cl(2)	94.6(2)
N−Fe−N(1A)[1]	75.0(3)	N(1A)[1]−Fe−Cl(1)	163.4(2)
N−Fe−Cl(1)	90.0(2)	N(1A)[1]−Fe−Cl(1)[1]	88.8(2)
N−Fe−Cl(1)[1]	90.0(2)	N(1A)[1]−Fe−Cl(2)	94.6(2)
N−Fe−Cl(2)	166.2(3)	Cl(1)−Fe−Cl(1)[1]	98.6(2)
N(1A)−Fe−N(1A)[1]	80.5(4)	Cl(1)−Fe−Cl(2)	98.99(12)
N(1A)−Fe−Cl(1)	88.8(2)	Cl(3)−Fe−Cl(2)	98.99(12)
N(1A)−Fe−Cl(1)[1]	163.4(2)		

[a] Superscript 1 indicates equivalent atom position.

[Fe(BPA)Cl_3] (2). The asymmetric unit of the crystal is characterized by two mononuclear neutral molecules which are linked by two intermolecular hydrogen bonds between an amine nitrogen of one molecule and a chloride of the other. The Fe−N_{amine} bond lengths, 2.223(7) and 2.197(7) Å, are longer than the Fe(III)−NH bond lengths found in (hexaamine)iron(III) low-spin complexes.[16] They are significantly shorter than those found in the [{Fe(bis(2-benzimidazolylmethyl)amine)(PhCOO)}$_2$O](ClO_4)$_2$ complex (average 2.286 Å).[17] The aver-

(15) Nakamoto, K. In *Infrared and Raman Spectra of Inorganic and Coordination Compounds*; Wiley: New York, 1986; pp 231−233.

(16) Bernhardt, P. V.; Comba, P.; Hambley, T. W.; Lawrance, G. A. *Inorg. Chem.* **1991**, *30*, 942−946.

(17) Gomez-Romero, P.; Casan-Pastor, N.; Ben-Hussein, A.; Jameson, G. B. *J. Am. Chem. Soc.* **1988**, *110*, 1988−1990.

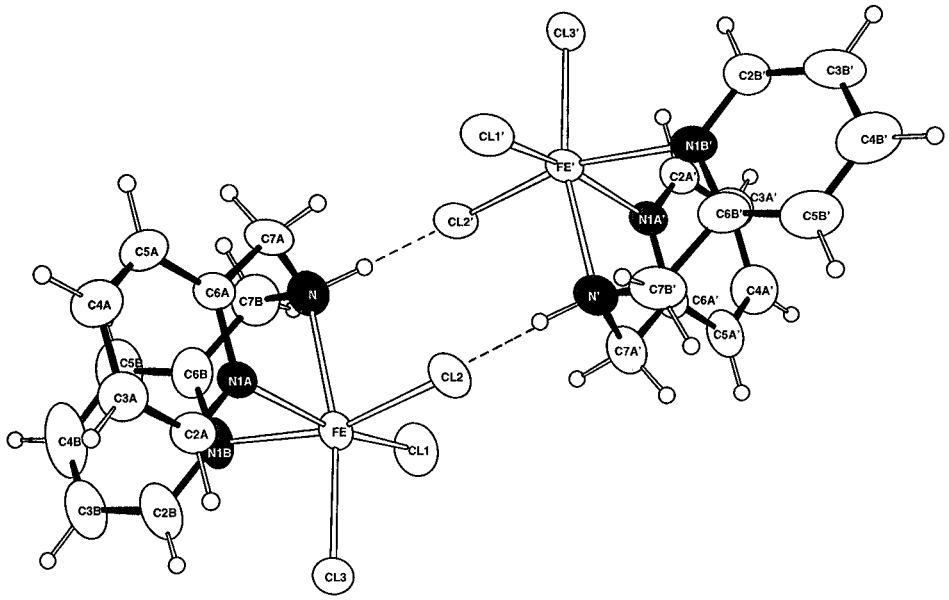

Figure 2. ORTEP view of $[Fe(BPA)Cl_3]$ (**2**) showing 50% probability thermal ellipsoids and the atom-labeling scheme.

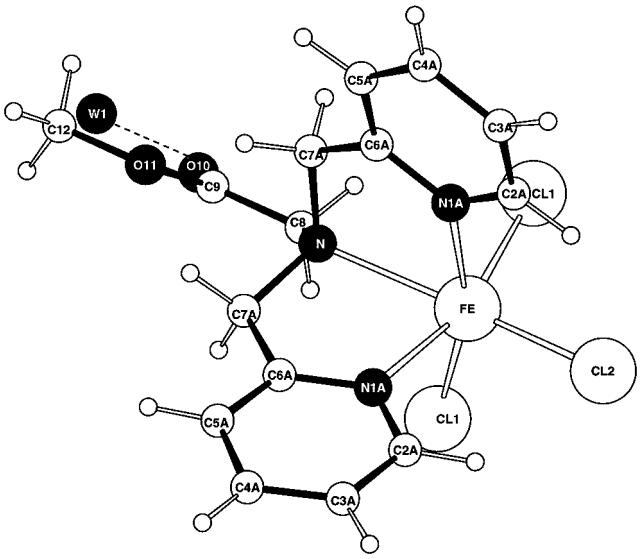

Figure 3. ORTEP view of $[Fe(BPE)Cl_3]$ (**3**) showing 50% probability thermal ellipsoïds and the atom-labeling scheme.

age bond length between iron and pyridine nitrogens is 2.190 Å, which is slightly longer than those found for $[Fe(BPG)DBC]^{2-}$ (2.143 Å).[6b] The distorsion in the coordination geometry is reflected in the bond angles. The average of the $N_{amine}-Fe-N_{py}$ angles (76.5°) is much lower than the ideal 90° value, due to the constraints imposed by the bipodal ligand arrangement. Also, the $N_{py}-Fe-N_{py}$ angle is 79.2° rather than 90° as expected for an ideal octahedron. The N−Fe−Cl angles are much closer to the ideal value of 90° because of the absence of constraint for the chloride position.

$[Fe(BPE)Cl_3]$ (3). Complex **3** is symmetric. The iron(III) center, one chloride anion, the amine nitrogen, and the three atoms of the carboxylate group are located in special positions in the mirror plane. One crystallized water molecule can also be observed in this mirror plane and is hydrogen bonded to the −C═O group of the ester function not involved in the coordination of the metal.

The bond length between iron and pyridine nitrogens (2.194-(8) Å) is very similar to the former ones. The distorsion in the coordination geometry is also due to the constraints imposed by the ligand arrangement which forms five-membered chelate rings. The major difference between $[Fe(BPA)Cl_3]$ and $[Fe(BPE)Cl_3]$ is the relative length of the $Fe-N_{amine}$ bonds. The latter is 2.337(11) Å in **3** which is significantly longer than the one found in **2** (2.2 Å). This can be related to the withdrawing character of the ester group.

Cleavage Mechanism. If N-dealkylation of the BPG ligand occurs as an oxidative cleavage, we should observe the formation of not only BPA but also the glyoxylic acid.[18] In order to identify this byproduct, we recorded ^1H NMR spectra of $[Fe(BPG)Cl_2]$ and $[Fe(BPA)Cl_3]$ in deoxygenated D_2O. The spectra showed isotropic shifts due to delocalization of the unpaired spin density, but these shifts were lower than expected for high-spin iron(III) molecules.[19] No signal was observed at a shift higher than 16 ppm. Both spectra are very similar. The $[Fe(BPG)Cl_2]$ spectrum, recorded in the absence of oxygen, shows that the complex is quite stable, but in presence of dioxygen, the spectrum evolves to yield a signal at 5 ppm. This signal is assigned to the aldehydic proton of the glyoxylic acid which is known to be observed at a chemical shift of 5 ppm.

The formation of glyoxylic acid was also investigated by GC mass spectrometry . Due to its high polarity we did not succeed in characterizing it directly. By reaction with diazomethane, we obtained its methylated derivative as the ($CH_3-CO-CO-OCH_3$) methyl pyruvate which is a less polar molecule. A 2 week old aqueous solution of $[Fe(BPG)Cl_2]$ was lyophilized, and a solution of diazomethane in diethyl ether was added to the residue at room temperature. The resulting solution was injected in the GC mass spectrometer. One fraction gave characteristic peaks for the methyl pyruvate (*m*/*e*): $M^+ = 102$ (10.8); 59 (5.2); 43 (100). No peaks were detected when diazomethane was directly added to a suspension of $[Fe(BPG)Cl_2]$ in diethyl ether. These experiments confirm that glyoxylic acid is formed from cleavage of the BPG ligand when coordinated to iron in solution.

Hypothetically, we propose two different mechanisms to account for this cleavage, in either the absence or the presence of dioxygen. In the first one (Figure 4), cleavage is produced

(18) Rosenblatt, D. H.; Burrows, E. P. In *The Chemistry of Functional Groups, Supplement F*; Pataï, S., Ed.; Wiley: New York, 1982; Vol 2, pp 1085−1149.
(19) Holm, R. H.; Hawkins, C. J. In *NMR of Paramagnetic Molecules*; La Mar, G. N., Horrocks,W. D., Jr., Holm, R. H., Eds.; Academic Press: New York, 1973.

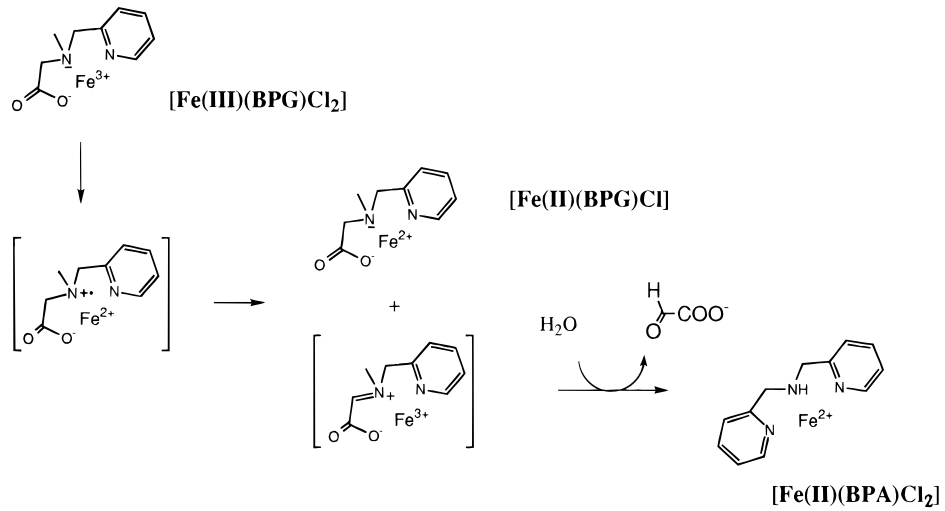

Figure 4. Anaerobic mechanism for the oxidative cleavage.

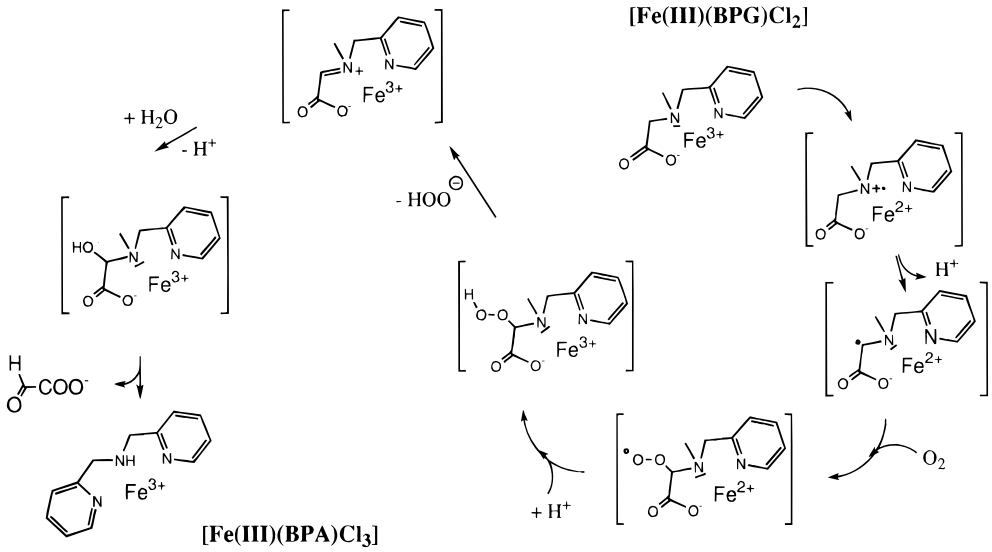

Figure 5. Aerobic mechanism for the oxidative cleavage.

anaerobically by disproportionation of [Fe(BPG)Cl_2] to yield two ferrous complexes [Fe^{II}(BPG)Cl] and [Fe^{II}(BPA)Cl_2] while the second ferrous complex results from subsequent intramolecular electron transfer and cleavage. This mechanism is very similar to that proposed for ligand dehydrogenation reported in the literature.[8] The second one (Figure 5), involving oxidation by dioxygen, yields only the [Fe^{III}(BPA)Cl_3] complex. Discrimination between the two mechanisms is quite difficult because of the sensitivity of the ferrous complexes to molecular dioxygen. Our results seem to favor the second one.

Electrochemical Studies and Reactivity with Dioxygen. Cyclic voltammograms of the complexes were recorded in acetonitrile under an argon atmosphere with 0.1 M Bu_4NPF_6. Preliminary studies on the reactivity with dioxygen were carried out in the case of [Fe(BPG)Cl_2] (**1**).[20]

The voltammetric behavior observed with **1**, illustrated in Figure 6, is clearly distinct from that of the ligand alone. The first redox system shown in the inset features the Fe(III)/Fe(II) couple in the complex. The potential location of this redox complex is similar to those of related complexes.[5,21] Exhaustive electrolysis showed also the iron(II) species to be stable under argon, so that various physical measurements could be carried out on this species. Besides the Fe(III)/Fe(II) redox couple, a second cathodic wave appears with a cathodic peak potential at −1.913 V. Two representative successive scans are presented. The full-line wave was recorded prior to the dashed

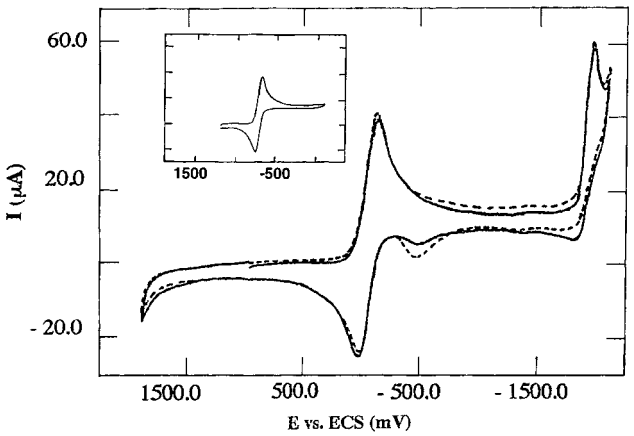

Figure 6. Cyclic voltammograms for 10^{-3} M [Fe(BPG)Cl_2] + 0.1 M Bu_4NPF_6 in acetonitrile. Scan rate: 200 mV/s. Solutions were thoroughly degassed with dry argon. Influence of repetitive scans on the reversibility of the second cathodic wave: Solid line, first scan up to the second cathodic wave; dashed line, second scan up to the second cathodic wave. Inset: Voltammogram restricted to the Fe(III)/Fe(II) couple.

(20) Sawyer, D. T. In *Oxygen Chemistry*; Oxford University Press: New York, Oxford, 1991.
(21) Nishida, Y.; Watanabe, I.; Unoura, K. *Chem. Lett.* **1994**, 1721−1724.

Table 5. Cyclic Voltammetry Characterization of Fe(III)/Fe(II) Redox Couples in CH_3CN + 0.1 M Bu_4NPF_6[a]

	$[Fe(BPG)Cl_2]$	$[Fe(BPA)Cl_3]$	$[Fe(BPE)Cl_3]$
E_{pc} (mV)	−90	−88	+4
ΔE_p (mV)	+104	+138	+281
$E°$ (mV)	−38	−19	+145

[a] Reference electrode: SCE.

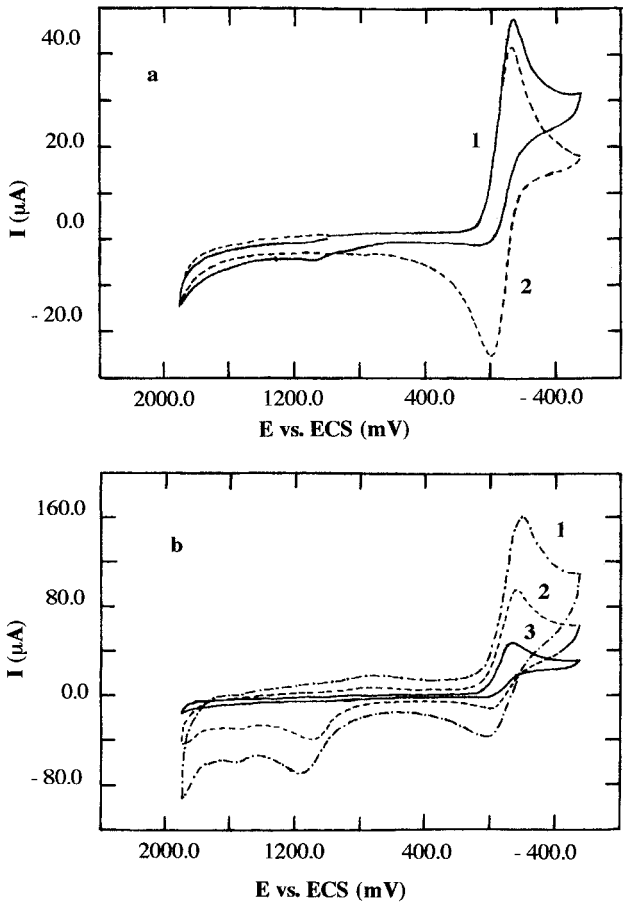

Figure 7. Cyclic voltammograms for 10^{-3} M $[Fe(BPG)Cl_2]$ + 0.1 M Bu_4NPF_6 in acetonitrile: (a) curve 1, influence of dioxygen on the first redox couple of $[Fe(BPG)Cl_2]$, and curve 2, cyclic voltammogram in the presence of argon added for the sake of comparison; (b) influence of the scan rate in the presence of dioxygen (curve 1, 3 V/s; curve 2, 2 V/s; curve 3, 200 mV/s).

one. The part of the cyclic voltammogram featuring the Fe(III)/Fe(II) redox couple remained unaffected during the first several runs with any switching potential. Modifications appeared in the more cathodic wave. The full-line curve shows a slight chemical reversibility with another anodic peak, at −0.482 V. The dashed curve shows that the chemical reversibility diminishes while new anodic current increases. This observation would suggest the progressive buildup of a new species, at least during the first several runs.

Complexes **2** and **3** were studied in acetonitrile for the sake of comparison with the behavior of complex **1**. Table 5 summarizes the main cyclic voltammetry characteristics of the Fe(III)/Fe(II) system in these complexes, at a scan rate of 200 mV/s. We focused first on the variation of $E°$ values, which were taken as the average between the cathodic and anodic peak potentials. Clearly, the redox potential of complex **1** is the most negative of the series, and although it does not differ greatly from complex **2**, it gives support to the expected trend that decarboxylation of **1** should lessen the electron density in the system resulting in an easier reduction. The most remarkable observation is the redox potential of complex **3**, dramatically more positive than those of the other two complexes. More specific comparison with complex **2** can be understood on the following basis: crystallographic analysis indicates that the Fe−N bond is longer in complex **3** than in complex **2** because the electron-withdrawing effect of the ester group decreases the electron density on the nitrogen tripodal atom and therefore on the iron. This can explain the difference observed in the $E°$ values.

Reactivity of the $[Fe(BPG)Cl_2]$ Complex (1) with Dioxygen. The behavior of the Fe(III)/Fe(II) redox couple in the absence and presence of molecular dioxygen was compared. Figure 7a sketches this situation at a scan rate of 200 mV/s. In the presence of dioxygen, the reduction of Fe(III) to Fe(II) is no longer followed on potential reversal by any oxidation trace in the expected potential domain. A very small oxidation peak appears at 1.0 V. The chemical reversibility of the system is partially recovered at a scan rate of 1 V/s, and a larger oxidation peak is seen simultaneously at 1 V. Figure 7b, recorded in the presence of dioxygen in the medium, shows these variation effects of the scan rate on the chemical reversibility of the Fe(III)/Fe(II) system of complex **1**. All these observations indicate that molecular oxygen reacts with the Fe(II) state of complex **1** and removes it from the electrode surface. A new species is formed which is oxidized roughly at 1 V *vs* SCE.

Conclusion

We have discovered an interesting example of site-selective metal-assisted cleavage of a C−N bond in the nitrogen-centered tripodal BPG ligand which combines one carboxylate and two pyridines as pendant groups. We have shown that by this process the tetradentate ligand when coordinated to iron is transformed to a tridentate ligand (BPA) which retains only the two pyridines as pendant groups, while the initial carboxylate pendant group is transformed to glyoxylic acid. The corresponding iron(III)−BPA complex has been obtained and fully characterized. When the synthesis is performed in more acidic conditions, another iron(III) complex is formed with the tridentate ligand BPE which, in addition to two pyridines, presents the carboxylate group transformed into an ester and therefore no longer bound. Redox potentials corroborate the structural features for the reported complexes. All results given here suggest that the reaction is initiated by a slow intramolecular redox process in which iron(III) and the ligand are oxidant and reductant, respectively. Preliminary electrochemical results on the reaction of the $[Fe(BPG)Cl_2]$ complex in its reduced form with dioxygen are given. Work in progress is aimed at the elucidation of various reactivities and the characterization of possible transient species in a series of the closely related non-heme iron models that we have discovered.

Acknowledgment. The authors acknowledge helpful comments by reviewers during revision of this paper. Dr. D. Mansuy and Dr. I. Artaud (Université Paris-V) are acknowledged for valuable discussions. We appreciate the kind editing of this paper by R. Green Beau.

Supporting Information Available: Tables of crystallographic and experimental data, atomic coordinates, anisotropic thermal parameters, hydrogen coordinates, and bond lengths and angles for $[Fe(BPA)Cl_3]$ and $[Fe(BPE)Cl_3]$ (14 pages). Ordering information is given on ay current masthead page.

IC961369L